High-Temperature Superconductivity without the Effect of Antiferromagnetism Observed in Electron-Doped Cuprate Superconductors

Since the discovery of cuprate high-temperature superconductors, the nature of antiferromagnetism in cuprates has been extensively studied. Especially for electron-doped cuprate superconductors, antiferromagnetic order is so robust that it has been believed to persist even in the superconducting phase. By angle-resolved photoemission spectroscopy measurement of single crystals of electron-doped cuprates, we have demonstrated that sufficient reduction annealing suppresses antiferromagnetism while maintaining a high superconducting transition temperature. The present result fundamentally challenges the physics of high-temperature superconductivity and calls for a re-examination of the relationship between superconductivity and antiferromagnetism.

The relationship between antiferromagnetism and superconductivity has been one of the central issues in cuprate superconductors. Doping carriers into antiferromagnetic (AFM) and Mott-insulating parent compounds induces superconductivity, but the AFM order is so robust that it persists even in the superconducting state in electron-doped cuprate high-temperature superconductors (e-HTSCs). Strong AFM correlation manifests itself as the opening of a band gap at the "hot spot" where the Fermi surface (FS) and the Brillouin zone folded by the AFM order cross with each other. This band gap, called AFM pseudogap, has been seen in all e-HTSCs so far [1] and hence antiferromagnetism has been regarded as an essential ingredient in e-HTSCs.

Since the discovery of e-HTSCs, it has been known that electron doping alone cannot induce superconductivity, and annealing in a reducing atmosphere is indispensable [2]. As-grown samples are non-superconducting and AFM. By annealing, impurity oxygen atoms which stabilize the AFM order are removed and superconductivity appears. Recently, superconductivity was found in thin films [3, 4] or powdered samples [5, 6] of e-HTSCs even without electron doping by Ce substitution. The large surface-to-volume ratio of thin films and powders probably makes the removal of the impurity oxygen atoms by annealing more effective. Inspired by those studies, Adachi *et al.* improved the annealing method for single crystals [7] and achieved superconductivity in $Pr_{1.3-x}La_{0.7}Ce_xCuO_4$ (PLCCO) down to the heavily underdoped (x = 0.05) region [8] where the sample had been believed to be an AFM insulator [9] (**Figs. 1a**, **b**).

In order to investigate the electronic structure of e-HTSCs annealed in this new method, which is called protect-annealing (**Fig. 1c**), we have performed angle-resolved photoemission spectroscopy (ARPES) measurements on single crystals of PLCCO with x = 0.10 [10]. We prepared three kinds of samples under different annealing conditions: as-grown, weakly protect-annealed and sufficiently protect-annealed samples, among which only the sufficiently annealed samples showed a superconducting transition temperature (T_c) of 27.0 K (**Fig. 1d**). ARPES measurements were carried out at BL-28A of the Photon Factory and at the Hiroshima Synchrotron Radiation Center.

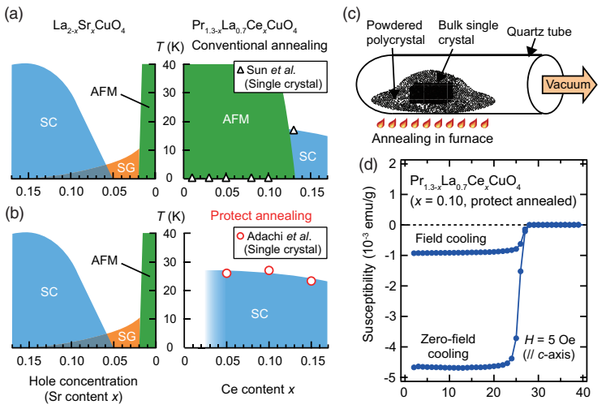

Figure 1: Superconducting properties of PLCCO samples. **(a)** T_c values determined from the resistivity of PLCCO single crystals annealed by the conventional method reported by Sun *et al.* (open triangles) [9]. The AFM, superconducting, and spin-glass phases are denoted by AFM, SC, and SG, respectively. A typical phase diagram for a hole-doped cuprate $La_{2-x}Sr_xCuO_4$ is also shown on the left-hand side. **(b)** The same plot as **(a)** for protect-annealed single crystals reported by Adachi *et al.* (open circles) [7, 8]. T_c was determined from magnetic susceptibility measurements. **(c)** Schematic description of the protect-annealing method. **(d)** Magnetic susceptibility of a protect-annealed PLCCO single crystal which shows T_c of 27.0 K.

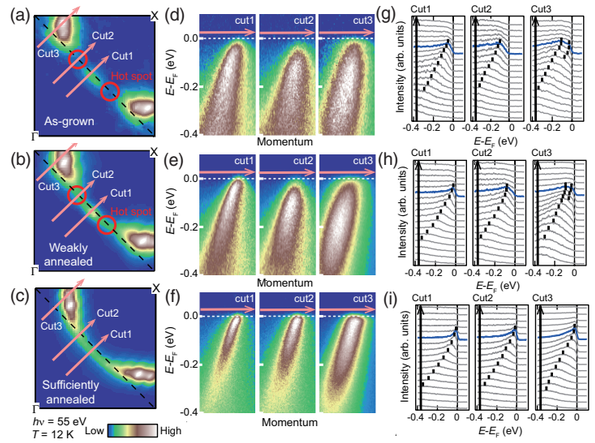

Figure 2: ARPES spectra of PLCCO. **(a)-(c)** FS mappings of as-grown, weakly annealed, and sufficiently annealed samples, respectively. **(d)-(f)** Band image for each sample along the cuts indicated in **(a)-(c)**. **(g)-(i)** EDCs plotted for each cut. Blue EDCs are taken at the Fermi wave vectors.

Figures 2a-c show FS mapping of as-grown, weakly annealed, and sufficiently annealed samples. In the as-grown sample, intensity around the hot spot, indicated by red circles, is strongly suppressed due to the presence of the AFM order. The intensity partially recovers by weak annealing, but the FS is still disconnected at the hot spot, suggesting that the annealing was not enough and strong AFM correlation still persists. However, sufficient annealing dramatically changes the situation. The suppressed intensity is fully recovered and the FS becomes continuous in the entire momentum space. Changes induced by the protect-annealing can also be seen in the band images (**Figs. 2d-f**) and corresponding energy distribution curves (EDCs) (**Figs. 2g-i**) plotted along the cuts indicated in **Figs. 2a-c**. For the as-grown and weakly annealed samples, the quasi-particle (QP) peak is shifted toward higher binding energy at the hot spots (cut 2), and the QP peak splits around the antinode (cut 3) due to the strong AFM correlation. However, by sufficient annealing, the band gap closes and a single QP peak is observed on the entire FS. These results suggest that protect-annealing strongly suppressed the antiferromagnetism, specifically, AFM correlation length and/or magnitude of the local magnetic moment.

Assuming Luttinger's theorem, we estimated electron concentration from the area of the FSs and found that the amount of doped electrons in sufficiently annealed samples ranged from 0.118 to 0.180, larger than the nominal Ce concentration x = 0.10. The origin of the additional electron doping by annealing could be the removal of oxygen atoms from the regular sites. Although electron doping by Ce substitution rapidly degrades superconductivity and reduces the size of the superconducting dome in the phase diagram [1, 11], the present protect-annealed samples show high T_c in a much wider electron concentration range in the absence of the AFM pseudogap. This observation calls for a re-examination of the relationship between superconductivity and antiferromagnetism and of the phase diagram of e-HTSCs.

REFERENCES

[1] H. Matsui, T. Takahashi, T. Sato, K. Terashima, H. Ding, T. Uefuji and K. Yamada, *Phys. Rev. B* **75**, 224514 (2007).
[2] Y. Tokura, H. Takagi and S. Uchida, *Nature* **337**, 345 (1989).
[3] A. Tsukada, Y. Krockenberger, M. Noda, H. Yamamoto, D. Manske, L. Alff and M. Naito, *Solid State Commun.* **133**, 427 (2005).
[4] O. Matsumoto, A. Utsuki, A. Tsukada, H. Yamamoto, T. Manabe and M. Naito, *Phys. C* **469**, 924 (2009).
[5] S. Asai, S. Ueda and M. Naito, *Phys. C* **471**, 682 (2011).
[6] T. Takamatsu, M. Kato, T. Noji and Y. Koike, *Appl. Phys. Express* **5**, 073101 (2012).
[7] T. Adachi, Y. Mori, A. Takahashi, M. Kato, T. Nishizaki, T. Sasaki, N. Kobayashi and Y. Koike, *J. Phys. Soc. Jpn* **82**, 063713 (2013).
[8] T. Adachi *et al.*, unpublished.
[9] X. F. Sun, Y. Kurita, T. Suzuki, S. Komiya and Y. Ando, *Phys. Rev. Lett.* **92**, 047001 (2004).
[10] M. Horio, T. Adachi, Y. Mori, A. Takahashi, T. Yoshida, H. Suzuki, L. C. C. Ambolode II, K. Okazaki, K. Ono, H. Kumigashira, H. Anzai, M. Arita, H. Namatame, M. Taniguchi, D. Ootsuki, K. Sawada, M. Takahashi, T. Mizokawa, Y. Koike and A. Fujimori, *Nat. Commun.* **7**, 10567 (2016).
[11] T. Uefuji, K. Kurahashi, M. Fujita, M. Matsuda and K. Yamada, *Phys. C* **378–381**, 273 (2002).

BEAMLINE

BL-28A

M. Horio[1], T. Adachi[2], Y. Mori[3], A. Takahashi[3], T. Yoshida[1], H. Suzuki[1], L. C. C. Ambolode II[1], K. Okazaki[1], K. Ono[4], H. Kumigashira[4], H. Anzai[5], M. Arita[5], H. Namatame[5], M. Taniguchi[5], D. Ootsuki[1], K. Sawada[1], M. Takahashi[1], T. Mizokawa[1], Y. Koike[3] and A. Fujimori[1] ([1]The Univ. of Tokyo, [2]Sophia Univ., [3]Tohoku Univ., [4]KEK-IMSS-PF, [5]Hiroshima Synchrotron Radiation Center)